Supplemental Material for

[Influence of aluminum on the elasticity of majorite-pyrope garnets]

Zhaodong Liu [1, 2 *], Steeve Gréaux [3], Nao Cai [4], Nicki Siersch [1], Tiziana Boffa Ballaran [1], Tetsuo Irifune [3], Dan J. Frost [1]

1. Bayerisches Geoinstitut, University of Bayreuth, 95440 Bayreuth, Germany
2. State Key Laboratory of Superhard Materials, Jilin University, Changchun 130012, China
3. Geodynamics Research Center, Ehime University, Matsuyama 790-8577, Japan
4. Mineral Physics Institute, Stony Brook University, Stony Brook, NY 11794, USA

Supplemental Material includes the standard error analysis, two-way travel times of P- and S-wave of the $Mj_{90}Py_{10}$ and $Mj_{59}Py_{41}$ garnet as a function of the collected frequency (Figure S1), the linear fitting of the density and elastic moduli with errors as a function of the garnet composition (Figure S2), and the table of the sample length and two-way travel times (Table S1)

Standard error analysis:

The velocity is derived from the following equation:

$$V_{P/S} = \frac{\mathrm{L}}{t_{P/S}} \quad (1)$$

where $V_{P/S}$ is the compression or shear velocity, L is the sample length, and $t_{P/S}$ is the travel time in the sample. The bulk and shear modulus can be further derived from their velocity and density (ρ)

$$K_S = \rho \cdot (V_p^2 - 4V_s^2/3) \quad (2)$$

$$G = \rho \cdot V_s^2 \quad (3)$$

The standard propagation errors (δ) for the above equations:

$$\frac{\delta_{V_{P/S}}}{V_{P/S}} = \sqrt{(\frac{\delta_L}{L})^2 + (\frac{\delta_{t_{P/S}}}{t_{P/S}})^2} \quad (4)$$

$$\frac{\delta_{K_S}}{K_S} = \sqrt{\left(\frac{\delta_\rho}{\rho}\right)^2 + \left(\frac{2\delta_{V_P}}{V_P}\right)^2 + \left(\frac{2\delta_{V_S}}{V_S}\right)^2} \quad (5)$$

$$\frac{\delta_G}{G} = \sqrt{(\frac{\delta_\rho}{\rho})^2 + (\frac{2\delta_{V_S}}{V_S})^2} \quad (6)$$

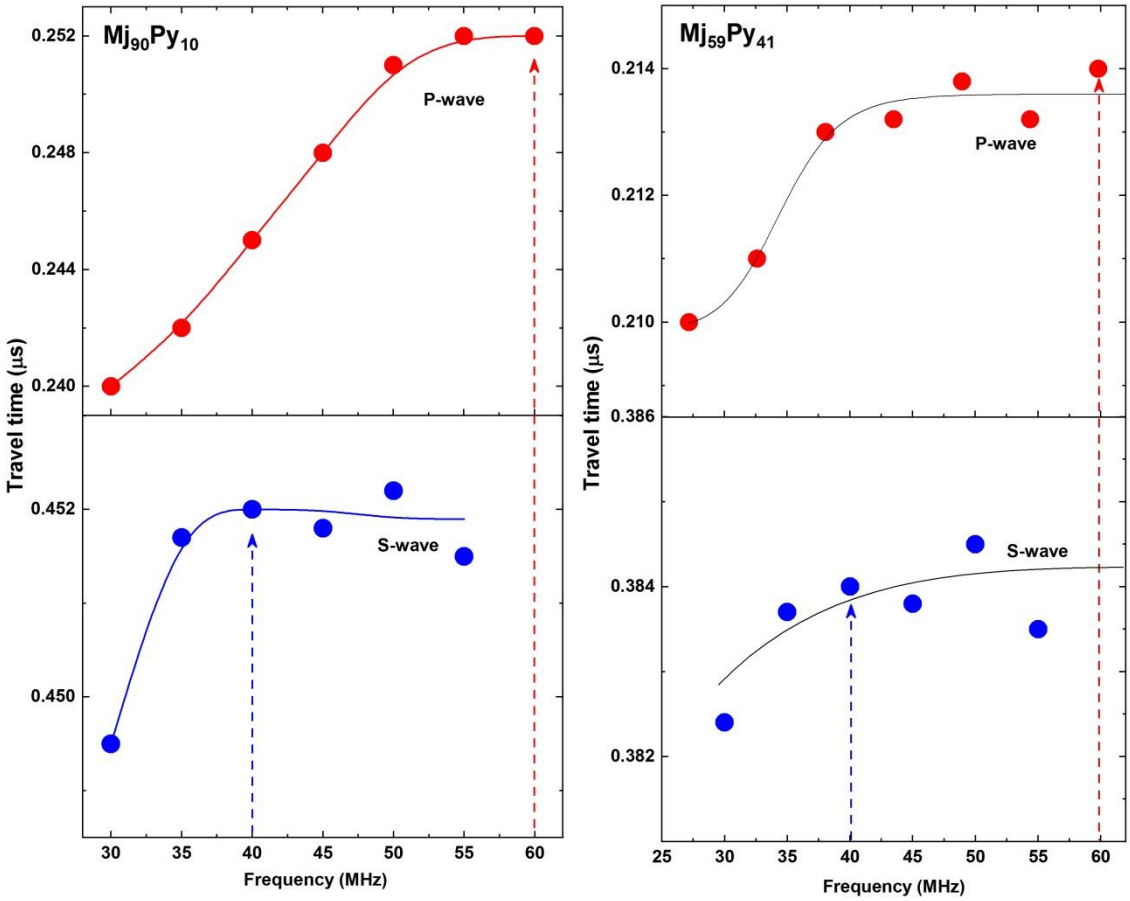

Figure S1 Two-way travel times of P- and S-wave for the $Mj_{90}Py_{10}$ and $Mj_{59}Py_{41}$ garnet as a function of the collected frequency. For $Mj_{90}Py_{10}$ garnet, we can see some frequency dependence of travel times for P-wave because the signal quality of the P-wave is not so good with frequencies, while the S-wave shows almost independent travel time with frequencies. This situation may be related with the quality of attaching $LiNbO_3$ transducers on the surface of the buffer rod due to a slightly difference of temperature or press load. Most samples show their travel times for both P- and S-wave are almost independent of frequencies, for example, $Mj_{59}Py_{41}$ in Figure S1. At 60 MHz, the P-wave signal is the strongest, while S-wave becomes bad and weak. So we can only derive the travel time of P-wave at 60 MHz for all the samples. In the present study, we collected travel times from 25 to 60 MHz for all the samples. To reduce the analytical uncertainty, we therefore adapted 60 MHz for P-wave and 40 MHz for S-wave to derive the travel time for all the samples.

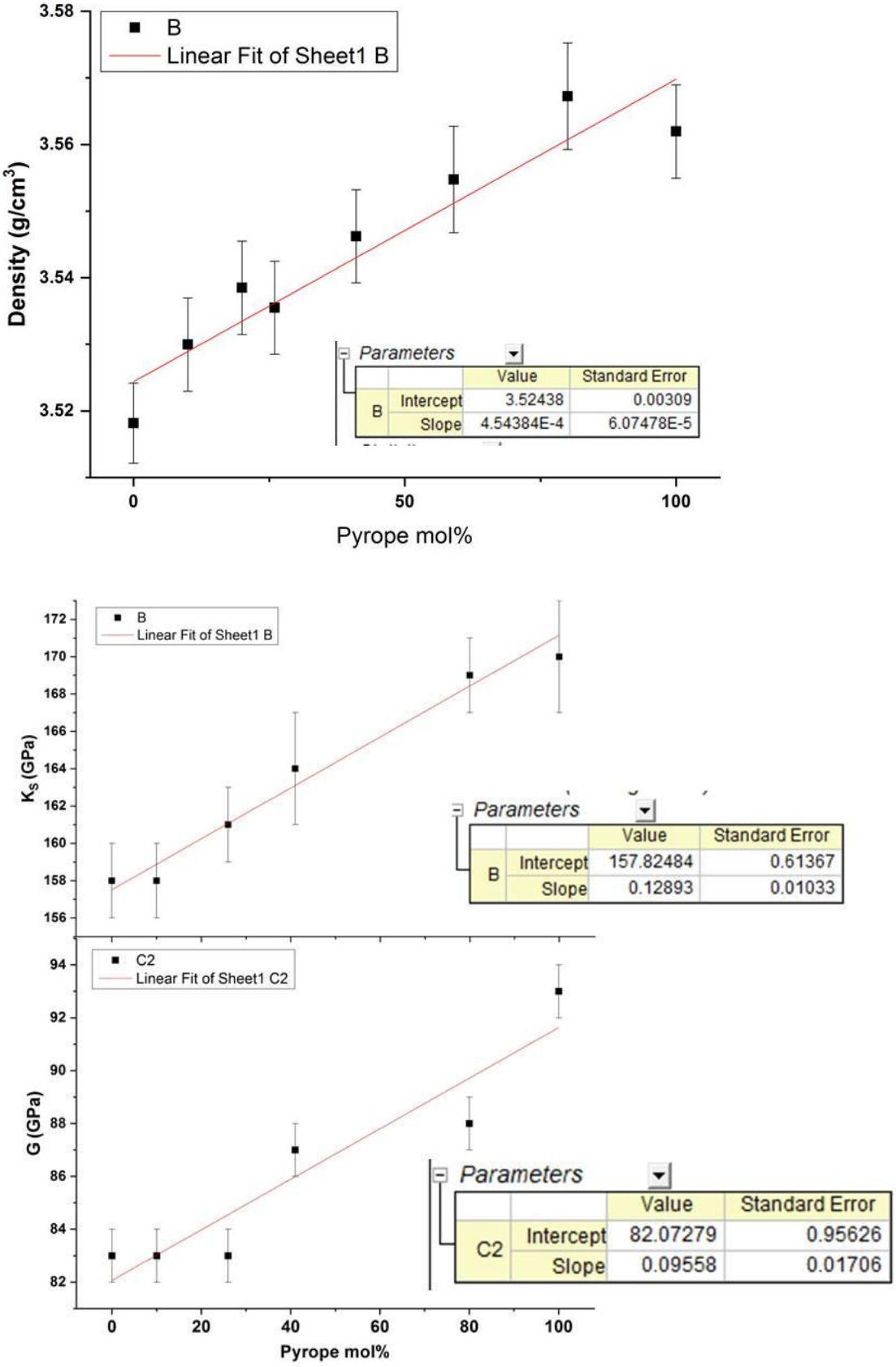

Figure S2. The linear fitting of the density and elastic moduli with errors as a function of the garnet composition for equation (1), (4), and (5) in the main text.

Table S1 The sample length and two-way travel times

Composition	Sample length L (mm)	$2t_P$ (μs)	$2t_S$ (μs)
Pyrope	1.075 (1)	0.237 (3)	0.422 (3)
$Mj_{20}Py_{80}$	1.059 (1)	0.331 (3)	0.596 (3)
$Mj_{59}Py_{41}$	0.953 (1)	0.214 (3)	0.384 (3)
$Mj_{74}Py_{26}$	1.196 (1)	0.273 (3)	0.494 (4)
$Mj_{90}Py_{10}$	1.098 (1)	0.252 (3)	0.452 (3)
Majorite	1.487 (1)	0.340 (3)	0.612 (3)